Bioorg. Med. Chem. Lett. 36 (2021) 127819

Contents lists available at ScienceDirect

Bioorganic & Medicinal Chemistry Letters

journal homepage: www.elsevier.com/locate/bmcl

# Structure based design, synthesis, and biological evaluation of imidazole derivatives targeting dihydropteroate synthase enzyme

Drashti G. Daraji [a], Dhanji P. Rajani [b], Smita D. Rajani [b], Edwin A. Pithawala [c], Sivaraman Jayanthi [d], Hitesh D. Patel [a,*]

[a] Department of Chemistry, School of Sciences, Gujarat University, Navarangpura, Gujarat, India
[b] Microcare Laboratory and TRC, Surat, India
[c] Microbiology and Biotechnology, Khyati Institute of Science, Palodia, Ahmedabad, Gujarat, India
[d] School of Bio Sciences and Technology, Vellore Institute of Technology, Vellore, Tamil Nadu, India

ARTICLE INFO

*Keywords:*
Imidazole
Antiresistant bacterial strains
saDHPS
Molecular docking
ADME

ABSTRACT

In this study, we have designed and synthesized 2-((5-acetyl-1-(phenyl)-4-methyl-1*H*-imidazol-2-yl)thio)-*N*-(4-((benzyl)oxy)phenyl) acetamide derivatives. Antimicrobial activities of all the imidazole derivatives have been examined against Gram-positive and Gram-negative bacteria and results showed that the conjugates have appreciable antibacterial activity. Besides, several analogous were evaluated for their *in vitro* antiresistant bacterial strains such as Extended-spectrum beta-lactamases (ESBL), Vancomycin-resistant *Enterococcus* (VRE), and Methicillin-resistant *Staphylococcus aureus* (MRSA). The SAR revealed that the 12l compound resulted in potency against all bacterial strains as well as ESBL, VRE, and MRSA strains. Lipinski's rule of five, and ADME studies were preformed for all the synthesized compounds with *Staphylococcus aureus* dihydropteroate synthase (saDHPS) protein (PDB ID: 6CLV) and were found standard drug-likeness properties of conjugates. Moreover, the binding mode of the ligands with the protein study has been examined by molecular docking and results are quite promising. Besides, all the analogous were tested for their *in vitro* antituberculosis, antimalarial, and antioxidant activity.

Infectious microbial disease remains a pressing crisis at worldwide, due to inaccurate diagnosis and increasing use or abuse of antibacterial agents as well as lack of development of new classes of antibacterial drugs.[1,2] Therefore, problems of multidrug-resistant (MDR) microorganisms have become an alarming point in many countries around the world.[3–5] In drug-resistant microbes, vancomycin-resistant, MRSA, and azole-resistant *Candida* species are familiar examples. Mostly, infections treatment caused to complicate by these microbes especially in the case of immune-compromised patients.[6] Resistance can arise either through the appearance of new strains that fall outside of compounds or the attainment of specific mechanisms (target mutation, efflux, or drug modifying enzymes). Among all the organisms, *Staphylococcus aureus* displays extensive resistance profiles, specifically the MRSA.[7,8]

Worldwide, MRSA has become one of the major health threats for the last two decades. It has been projected that more than half percent of *Staphylococcus* infections are due to MRSA.[9] MRSA infections are classified into two major types, (i) hospital-acquired (HA) MRSA and (ii) community-acquired (CA) MRSA. HA-MRSA occurs in patients due to specific risk factors such as urine, lungs, bloodstream, and surgical sites, while CA-MRSA happens in healthy individuals that do not have affecting factors which primarily affects skin and skin structure infections.[10,11] MRSA resist all members of the β-lactam class of antibiotic, sulfamethoxazole-trimethoprim (Bactrim)[12] thereby disarming all previous mainstay treatment against *Staphylococcus aureus*.[13] From the last several years, VRE has emerged as a persistent nosocomial pathogen with exaggeration of resistant genes from other bacteria even.[14] Furthermore, recent studies suggest that targeting DHPS may be effective substitutes for the treatment of MRSA bacterial infections.[15]

Dihydropteroate synthase (DHPS) is recognized to be a validated drug target to obstruct folate production in bacterial cells. For the mechanism, DHPS specific enzyme catalyzes condensation between 7,8-dihydropterine pyrophosphate (DHPP) and p-aminobenzoic acid (PABA) to form tetrahydrofolate.[16–20] Consequently, sulfonamide[21,22] was competed with the main target of the natural substrate PABA to stop the folate synthesis.[23–27] Clinically speaking, the presence of PABA or sulfa drugs binding site close to the flexible protein loops that are

* Corresponding author.
*E-mail address:* drhiteshpatel1@gmail.com (H.D. Patel).

https://doi.org/10.1016/j.bmcl.2021.127819
Received 26 November 2020; Received in revised form 8 January 2021; Accepted 19 January 2021
Available online 26 January 2021

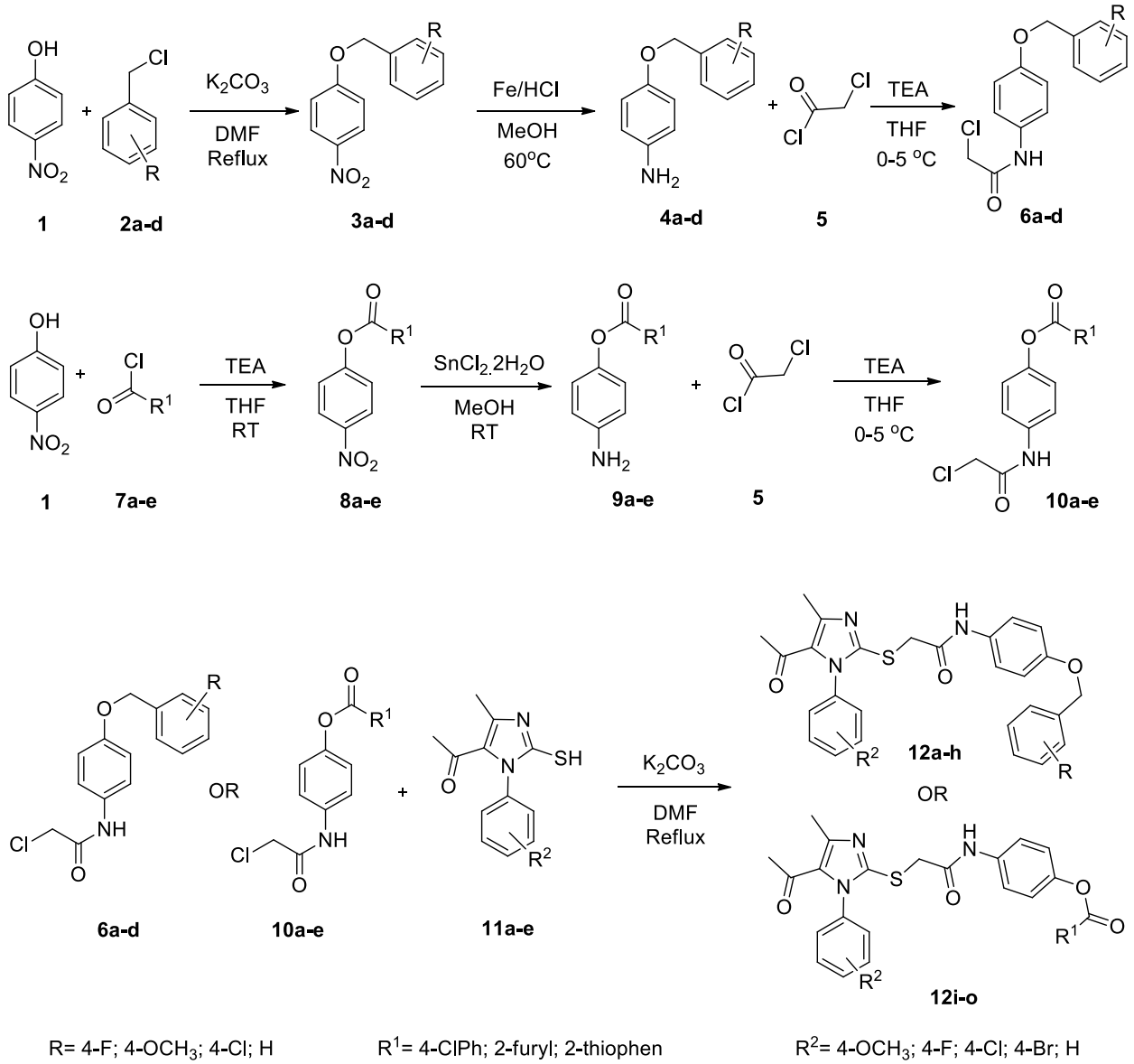


**Scheme 1.** Synthesis route of 2-((5-acetyl-1-(phenyl)-4-methyl-1*H*-imidazol-2-yl)thio)-*N*-(4-((benzyl)oxy)phenyl) acetamide derivatives.

agreeable and tolerant to mutations were the main drive toward this bacterial resistance,[28] but the predominant mechanism is mutation of the *folP* gene[29] that encodes DHPS.[30] Traditionally, the sulfonamides have been used for Gram-positive and Gram-negative bacterial infections,[21] combination with dihydropteroate reductase (DHFR) inhibitors such as trimethoprim which catalyzes an ensuing step in folate synthesis.[31,32]

Since 1940s, sulfonamides were the first successful antimicrobial agents and have been continuously used to treat a wide variety of bacterial infections such as *Toxoplasma gondii encephalitis*, *Pneumocystis jirovecii* pneumonia, *Staphylococcus aureus*,[33] and *Shigellosis*, and other disease like protozoal infections, malaria, and tuberculosis.[34] notwithstanding, its widespread application but found limited use of sulfa drugs against several infections attributable to rigorous immunological reactions and toxicity that causes fever, nausea, skin rashes, headache, breathing trouble, vomiting, loss of appetite, etc…[35] For that reason, urgent need to develop new approaches that can overcome the problems of microbial resistance.[36] So, discovery and developing a new class of antimicrobial agents are essential to fight against the increasing danger of drug-resistant microbes.[37,38] To discover new drugs, there are two main strategies; either to search for novel lead compounds or to modify the structure of a known drug.[23]

Using a structure-based approach, we have developed a novel lead series of analogous that displays micromolar inhibition of MRSA, ESBL, and VRE strains isolated from clinical samples. These compounds are characterized by various analytical methods like $^{1}$HNMR, mass, and IR spectroscopy. All conjugates were further tested against *in vitro* antimicrobial, antimalarial, antituberculosis, and antioxidant activities. For computational evaluation of all the analogous, analyses with Lipinski's rule of five (LRF), ADME and molecular docking study were exhibited.

We implemented a modest and efficient synthesis strategy to succeed the title compounds **(12a-12o)** as depicted in Scheme 1 (Table 1). Initial

**Table 1**
Synthesized 2-((5-acetyl-1-(phenyl)-4-methyl-1*H*-imidazol-2-yl)thio)-*N*-(4-((benzyl)oxy)phenyl) acetamide derivatives.

| Compound Code | R/R[1] | R[2] | Yield (%)[a] | Rection time (h) | M. P. (°C)[b] |
|---|---|---|---|---|---|
| **12a** | 4-F | 4-$OCH_3$ | 78 | 5.5 | 162.4 |
| **12b** | 4-F | 4-F | 72 | 5.0 | 181.7 |
| **12c** | 4-F | 4-Cl | 76 | 6.0 | 199.7 |
| **12d** | 4-$OCH_3$ | 4-Br | 68 | 6.5 | 193.0 |
| **12e** | 4-Cl | 4-Cl | 79 | 4.5 | 177.4 |
| **12f** | 4-Cl | H | 80 | 4.0 | 146.2 |
| **12g** | H | H | 73 | 4.0 | 181.7 |
| **12h** | H | 4-F | 71 | 4.5 | 200.7 |
| **12i** | 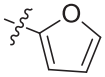 | 4-$OCH_3$ | 67 | 5.5 | 196.1 |
| **12j** | 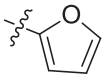 | 4-F | 70 | 4.0 | 197.6 |
| **12k** | 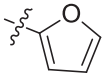 | 4-Br | 65 | 5.0 | 177.6 |
| **12l** | 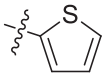 | 4-$OCH_3$ | 62 | 5.0 | 162.5 |
| **12m** | 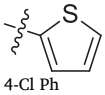 | 4-F | 69 | 4.5 | 177.7 |
| **12n** | 4-Cl Ph | 4-Br | 55 | 5.0 | 199.5 |
| **12o** | 4-Cl Ph | 4-Cl | 62 | 4.5 | 231.9 |

a: isolated yield.
b: melting point.

compounds 1-[1-(phenyl)-2-mercapto-4-methyl-1*H*-imidazol-5-yl]-ethanone **(11a-e)** were obtained from substituted aniline, 3-chloro-2,4-pentanedione, and potassium thiocyanate with good yield.[39] Treatment of p-nitro phenol **(1)** with benzyl chlorides **(2a-d)** in the presence of potassium carbonate yielded 1-(benzyloxy)-4-nitrobenzene **(3a-d)**. Reaction between p-nitro phenol **(1)** and benzoyl chloride **(7a-e)** were reacted using various catalysts such as potassium carbonate, triethyl amine (TEA) and different solvents like DMF, acetone, THF provided intermediate **(8a-e)**. However, triethyl amine (TEA) as a catalyst and THF as a solvent gave the good yield of compounds **(8a-e)**. Reduction of compounds **(3a-d)** or **(8a-e)** were performed using iron powder and hydrochloric acid (HCl) at 60 °C. Consequently, we had to use $SnCl_2{\cdot}2H_2O$ as a reducing agent for the synthesis of **(8a-e)** compounds at room temperature due to the presence of ester group in compounds. All the synthesized analogous were confirmed by the ninhydrin spray reagent on TLC. Finally, the following compounds **(4a-d)** or **(9a-e)** were reacted with chloro acetyl chloride **(5)** in a catalytic amount of triethyl amine (TEA) in THF to afford the *N*-(4-(benzyloxy)phenyl)-2-chloroacetamide **(6a-d)** or 4-(2-chloroacetamido)phenyl benzoate **(10a-e)** in good to excellent yield. The nucleophilic compound 1-[1-(phenyl)-2-mercapto-4-methyl-1*H*-imidazol-5-yl]-ethanone **(11a-e)**; sulfur group reacted with compounds **6a-d** or **10a-e** with potassium carbonate as a base catalyst to generate desire products **(12a-o)** in good yield. All the title analogous were well purified by the crystallization method using ethanol solvent.

Synthesized 2-((5-acetyl-1-(phenyl)-4-methyl-1*H*-imidazol-2-yl) thio)-*N*-(4-((benzyl)oxy)phenyl) acetamide compound was characterized by IR, $^1$H NMR, and mass spectroscopy after purification by crystallization using ethanol solvent. The appearance of characteristic absorption bands at 3294.21 and 1613.34 cm$^{-1}$ attributed to the stretching vibrations of –NH and –C═O, respectively noticeable the formation of amide via condensation of amine and chloroacetyl chloride. The IR spectrum of aromatic rings displayed peaks at 1546.10 and 1474.60 cm$^{-1}$ attributable to C═C stretching. Moreover, the appearance of a characteristic peak corresponding to C—N stretching in the region 1080–1360 cm$^{-1}$; in the IR spectra of imidazole provided evidence for the formation of imidazole ring. IR peak was observed at 1162.51 cm$^{-1}$ for C—O of compound contain ether group and showed at 1664 cm$^{-1}$ for C═O of ketone group. Peak 1096.73 cm$^{-1}$ observed due to the presence of C—S group. The IR spectrum of substituted ring displayed peaks at 1012.27 and 760.71 cm$^{-1}$ attributable to C–F and C–Cl stretching band, respectively. The $^1$H NMR spectrum of compound 12c peaks at; 8.924 ppm (s) showed the presence of –NH of CONH group. Compound displayed two singlet peaks in the region of 4.5–5.5 ppm due to the presence of two $CH_2$ functional groups. Molecular weight of **12c** is 523.11 g/mol (ChemDraw Ultra); which was confirmed by mass spectroscopy. It showed a molecular ion peak at *m/z* for 523.4 $[M]^+$, 524.4 $[M + 1]^+$, 525.4 $[M + 2]^+$.

All the synthesized compounds were tested for their antimicrobial activity and the results presented in Table 2. Interestingly, some of the imidazole derivatives displayed better antibacterial activity compared to standards. It is worth mentioning that all molecules exhibited significant activity against *Pseudomonas aeruginosa* and good to moderate activity against *Escherichia coli* and *Staphylococcus aureus* strains. Compounds **12a** and **12l** (12.5 μg/mL) showed more inhibition in *Escherichia coli* as compared to standard drug ciprofloxacin and **12c** (50 μg/mL) being equipotent to reference antibiotic chloramphenicol. Analogous **12f, 12h, 12j, 12k,** and **12m** displayed equipotent to ampicillin against *Escherichia coli* strain. Whereas *Streptococcus pyogenes* strain, analogous **12a, 12c, 12l,** and **12f** (12.5 μg/mL) were found to be more active than ciprofloxacin and **12d,** and **12g** (50 μg/mL) equipotent to chloramphenicol. Among all the compounds, derivatives **12h,** and **12j** were not found active and **12b, 12g,** and **12l** (62.5 μg/mL, 25 μg/mL, and 25 μg/mL, respectively) disclosed significant activity against *Staphylococcus aureus* strain. Analogous **12b** bearing 4-F substitution on both aryl rings showed less inhibition as compared to non-substituted **12g**. Compounds **12f** (62.5 μg/mL) and **12l** (50 μg/mL) showed good activity against *Streptococcus pyogenes*.

Derivatives of compound **12a,** and **12l** showed better results than other compounds, probably due to the presence of 4-$OCH_3$ substitution on aryl imidazole moiety. Similarly, compounds **12c** and **12f**, bearing 4-Cl aryl chain showed good antibacterial activity. Series of compounds, bearing benzyl chain displayed significant activity against antibacterial activity compared to benzoyl contained analogous. In the bacterial activity, **12l** compound exposed the best active in all the bacterial strains. Interestingly, compound **12l** bearing 4-$OCH_3$-aryl imidazole moiety, revealed a prominent inhibition pattern ranging from potent to considerable activity against the entire set of tested microorganisms. In this series, compound **12j**, bearing 4-F aryl imidazole moiety and furan substituted chain, showed the least antibacterial activity against all tested strains. Furthermore, analogous showed less active against antifungal strains. Compounds **12i** (250 μg/mL) derivatives bearing 4-$OCH_3$-aryl imidazole scaffold with furan side chain was the most active against *Candida albicans* compared to griseofulvin. Analogous **12a, 12b, 12d, 12g, 12j,** and **12m** were exhibited equipotent to griseofulvin against *Candida albicans* strain. Both side 4-Cl substituted **12o** derivative was displayed less active against all antifungal strains. SAR study clearly showed that compounds bearing 4-$OCH_3$-aryl imidazole moiety, i.e. **12a, 12l,** and **12i** displayed higher antimicrobial activity, probably due to the presence of donating substituent. 4-F-aryl imidazole moiety is more hydrophobic than other halo substituted groups. Comparison of

**Table 2**
Biological activity.

| Compound Code | Antibacterial activity | | | | Antifungal activity | | | Antituberculosis activity | Antimalarial Activity |
|---|---|---|---|---|---|---|---|---|---|
| | MIC[a] μg/mL | | | | MFC[b] μg/mL | | | | |
| | *EC*[d] | *PA*[e] | *SA*[f] | *SP*[g] | *CA*[h] | *AN*[i] | *AC*[j] | MIC[a] μg/mL | $IC_{50}^{c}$ μg/mL |
| **12a** | 12.5 | 25 | 100 | 100 | 500 | 500 | 500 | 50 | 1.40 |
| **12b** | 125 | 100 | 62.5 | 125 | 500 | 1000 | 500 | 100 | 0.82 |
| **12c** | 50 | 25 | 100 | 100 | 1000 | 1000 | 1000 | 62.5 | 0.73 |
| **12d** | 125 | 50 | 250 | 125 | 500 | >1000 | 1000 | 250 | 1.25 |
| **12e** | 250 | 125 | 100 | 100 | 1000 | >1000 | >1000 | 25 | 0.56 |
| **12f** | 100 | 25 | 250 | 62.5 | >1000 | 500 | 500 | 12.5 | 1.45 |
| **12g** | 125 | 50 | 25 | 125 | 500 | 1000 | 1000 | 500 | 0.93 |
| **12h** | 100 | 125 | 500 | 250 | 1000 | >1000 | >1000 | 62.5 | 0.45 |
| **12i** | 125 | 100 | 250 | 125 | 250 | >1000 | >1000 | 62.5 | 0.78 |
| **12j** | 100 | 250 | 500 | 250 | 500 | 500 | 500 | 250 | 0.36 |
| **12k** | 100 | 250 | 100 | 250 | 1000 | 500 | 500 | 25 | 1.18 |
| **12l** | 12.5 | 12.5 | 25 | 50 | 1000 | 500 | 500 | 25 | 0.45 |
| **12m** | 100 | 62.5 | 125 | 125 | 500 | 500 | 250 | 100 | 1.14 |
| **12n** | 125 | 100 | 250 | 100 | 1000 | 500 | 500 | 12.5 | 1.04 |
| **12o** | 250 | 100 | 125 | 100 | >1000 | >1000 | >1000 | 125 | 0.46 |
| **Gentamicin**[k] | 0.05 | 1 | 0.25 | 0.5 | – | – | – | – | – |
| **Ampicillin**[k] | 100 | 100 | 250 | 100 | – | – | – | – | – |
| **Chloramphenicol**[k] | 50 | 50 | 50 | 50 | – | – | – | – | – |
| **Ciprofloxacin**[k] | 25 | 25 | 50 | 50 | – | – | – | – | – |
| **Norfloxacin**[k] | 10 | 10 | 10 | 10 | – | – | – | – | – |
| **Nystatin**[k] | – | – | – | – | 100 | 100 | 100 | – | – |
| **Griseofulvin**[k] | – | – | – | – | 500 | 100 | 100 | – | – |
| **Isoniazid**[k] | – | – | – | – | – | – | – | 0.20 | – |
| **Chloroquine**[k] | – | – | – | – | – | – | – | – | 0.020 |
| **Quinine**[k] | – | – | – | – | – | – | – | – | 0.268 |

a: Minimum Inhibition Concentration.
b: Minimum Fungicidal Concentration.
c:Half maximal inhibitory concentration.
d: *Escherichia coli* (MTCC 443).
e: *Pseudomonas aeruginosa* (MTCC 1688).
f: *Staphylococcus aureus* (MTCC 96).
g: *Streptococcus pyogenes* (MTCC 442).
h: *Candida albicans* (MTCC 227).
i: *Aspergillus niger* (MTCC 282).
j: *Aspergillus clavatus* (MTCC 1323).
k: Standard drug.

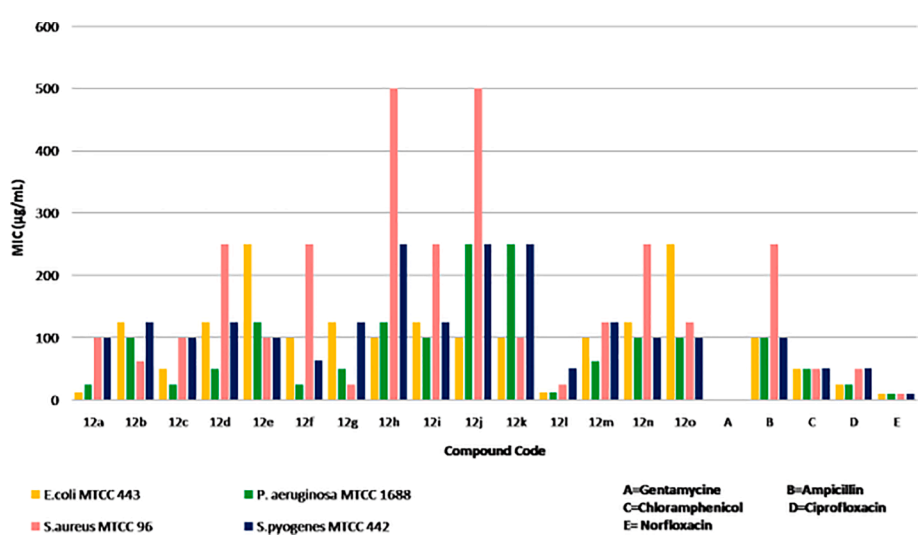


**Fig. 1.** Graphical representations of antibacterial and antifungal activity, respectively.

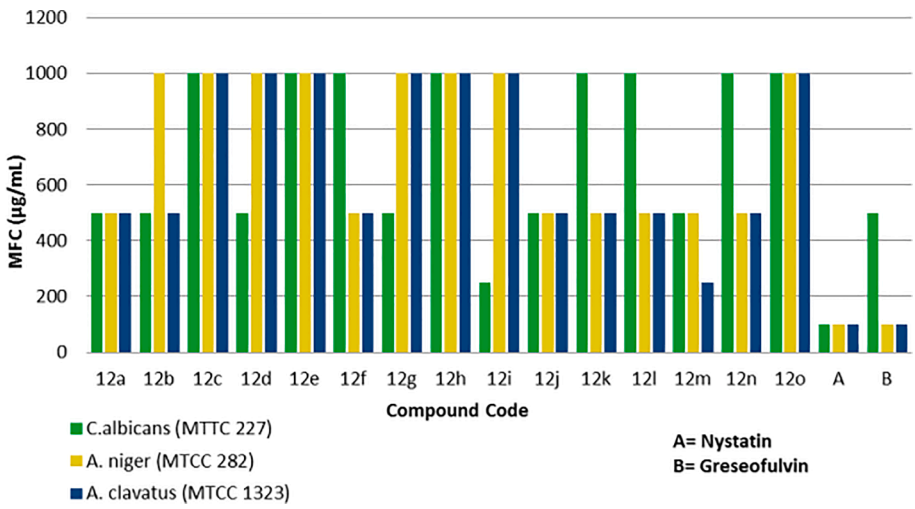


**Fig. 2.** Graphical representations of antibacterial and antifungal activity, respectively.

**Table 3**
Biological activity for resistant bacterial strains.

| Compound Code | Resisted bacterial strain | | |
|---|---|---|---|
| | Minimal Inhibition Concentration (µg/mL) | | |
| | ESBL[a] | VRE[b] | MRSA[c] |
| **12a** | 25 | 100 | 125 |
| **12b** | 250 | 125 | 100 |
| **12c** | 62.5 | 62.5 | 125 |
| **12d** | 250 | 250 | 500 |
| **12e** | 500 | 500 | 125 |
| **12f** | 125 | 100 | 100 |
| **12g** | 250 | 500 | 100 |
| **12h** | 125 | 250 | 1000 |
| **12i** | 500 | 250 | 500 |
| **12j** | 125 | 500 | 1000 |
| **12k** | 250 | 250 | 100 |
| **12l** | 62.5 | 100 | 100 |
| **12m** | 125 | 125 | 250 |
| **12n** | 250 | 500 | 500 |
| **12o** | 1000 | 500 | 500 |

a = Extended spectrum beta-lactamases.
b = Vancomycin-resistant *enterococci.*
c = Methicillin-resistant *Staphylococcus aureus.*

antibacterial and antifungal activity of compounds with reference drugs has been shown in Figs. 1 & 2.

In the primary study, all the synthesized compounds were found good active against *Escherichia coli* and *Staphylococcus aureus* strains then we had gone for further study of resisted bacterial strain against ESBL, VRE, and MRSA. All the bacterial strains were listed in Table 3. MIC values of all the targeted compounds were determined by the above-mentioned method at a micro-care laboratory, Surat. Firstly, compound **12a** with the MIC value 25 µg/mL and **12c, 12l** with the MIC value 62.5 µg/mL were found best active against ESBL strain. The analogous **12b, 12d, 12g, 12h, 12j, 12k, 12m,** and **12n** exhibited moderate antimicrobial activity against ESBL and VRE tested strains with MIC values 100, 125, and 250 µg/mL. Subsequently, **12c** derivative (62.5 µg/mL) was demonstrated excellent activity and compounds **12a, 12f,** and **12l** (100 µg/mL) were good active against VRE strain. Besides, MRSA tested strain was found less active as compared to other two resisted bacterial strains. Compounds **12b, 12f, 12g, 12k,** and **12l** were displayed good active for anti-MRSA. From all the tested compounds, **12l** bearing 4-$OCH_3$ aryl imidazole derivative found the best activity for the all resistant bacterial strains where **12o**, both side 4-Cl substitutions were brought into being the lowest activity. In general, 4th position of phenyl imidazole fragment increased the activity with the functional group such as 4-$OCH_3$ > 4-H > 4-Cl > 4-F > 4-Br. The resistant bacterial strains SAR of all synthesized compounds were mentioned in Fig 3.

All the tested molecules were not showing better activity than the standard drug to inhibit *H37Rv* strains in Table 2. All the synthesized compounds were evaluated for their *in vitro* antimalarial activity against *plasmodium falciparum*. All analogous were found to moderate activity against *plasmodium falciparum*. Among all the compounds, analogous **12h, 12j,** and **12l** were exhibited good activity as compared with reference drug Quinine (Table 2).

All synthesized titled compounds were more explored for their *in vitro* antioxidant property by 1,1-diphenylpicrylhydrazyl (DPPH), nitric oxide (NO), and hydrogen peroxide ($H_2O_2$) radical scavenging assay which was summarized in Table 4. Compounds **12h,** and **12o** showed inhibitory radical scavenging activity in all three methods due to the presence of mild electron-withdrawing groups. Though the DPPH radical scavenging abilities of all the imidazole derivatives were significantly lower than those of ascorbic acid (91.73 µg/ml), it was

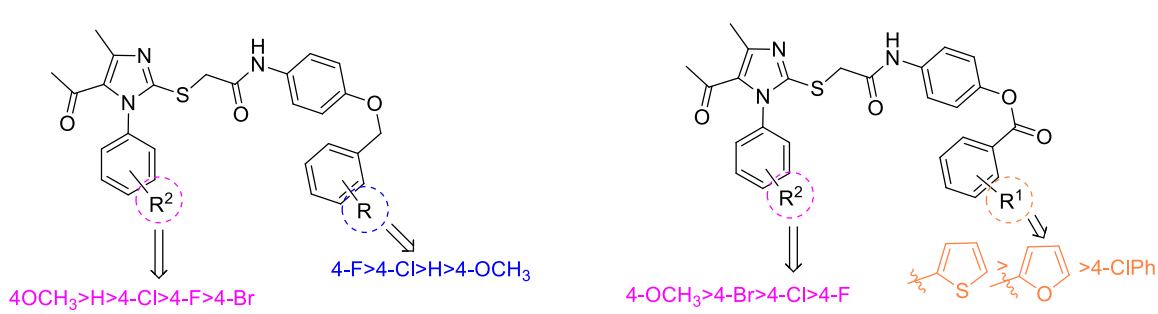


**Fig. 3.** The resistant bacterial strains SAR of all synthesized compounds.

**Table 4**
Antioxidant activity of synthesized compounds.

| No* | DPPH method | | | | | NO method | | | | | $H_2O_2$ method | | | | |
|---|---|---|---|---|---|---|---|---|---|---|---|---|---|---|---|
| | Concentration (μg/ml) | | | | | Concentration (μg/ml) | | | | | Concentration (μg/ml) | | | | |
| | 0 | 25 | 50 | 75 | 100 | 0 | 25 | 50 | 75 | 100 | 0 | 25 | 50 | 75 | 100 |
| **12a** | 26.4 | 31.6 | 54.2 | 67.2 | 84.3 | 34.0 | 45.8 | 63.4 | 81.4 | 90.5 | 32.4 | 54 | 68.1 | 79.8 | 84.3 |
| **12b** | 22.0 | 34.8 | 56.4 | 71.6 | 89.4 | 36.4 | 46.8 | 60.4 | 70.3 | 89.6 | 29.5 | 46.1 | 53.4 | 63.1 | 71.2 |
| **12c** | 31.0 | 42.9 | 58.6 | 67.0 | 91.0 | 40.5 | 50.8 | 58.3 | 84.3 | 89.5 | 34.0 | 51.0 | 68.4 | 74.5 | 88.1 |
| **12d** | 26.1 | 34.8 | 41.3 | 59.7 | 73.2 | 40.5 | 51.7 | 65.4 | 75.3 | 84.3 | 31.4 | 47.0 | 60.7 | 71.0 | 84.3 |
| **12e** | 31.4 | 41.2 | 51.7 | 58.6 | 85.7 | 41.6 | 47.3 | 64.3 | 80.6 | 88.8 | 26.3 | 47.8 | 59.4 | 75.2 | 89.7 |
| **12f** | 28.4 | 52.1 | 68.2 | 76 | 84.7 | 35.8 | 49.5 | 61.4 | 76.9 | 88.4 | 36.1 | 42.6 | 59.4 | 67.3 | 79.6 |
| **12g** | 26.4 | 36.4 | 48.6 | 60.0 | 84.3 | 37.9 | 48.3 | 64.2 | 80.3 | 87.4 | 31.6 | 43.8 | 58.0 | 69.4 | 81.9 |
| **12h** | 27.9 | 46.8 | 56.2 | 62.3 | 84.7 | 35.7 | 45.7 | 60.8 | 72.4 | 85.9 | 28 | 47.4 | 63.7 | 84.0 | 91.8 |
| **12i** | 28.1 | 32.5 | 47.1 | 66.2 | 85.2 | 25.8 | 37.7 | 59.3 | 78.9 | 84.5 | 39.2 | 59.3 | 69.9 | 81.0 | 90.0 |
| **12j** | 27.5 | 34.6 | 48.2 | 66.7 | 82.1 | 34.2 | 45.2 | 67.4 | 79.6 | 81.7 | 43.1 | 55.9 | 64.8 | 76.5 | 85.1 |
| **12k** | 33.3 | 43.2 | 57.1 | 64.8 | 88.7 | 28.7 | 49.3 | 65.3 | 75.8 | 86.7 | 32.8 | 51.7 | 68.7 | 79.0 | 86.5 |
| **12l** | 28.1 | 46.8 | 56.1 | 68.1 | 81.6 | 29.8 | 42.3 | 69.1 | 76.8 | 81.7 | 27.3 | 39.4 | 61.0 | 76.4 | 82.3 |
| **12m** | 34.7 | 44.3 | 51.4 | 65.4 | 89.6 | 40.3 | 50.6 | 59.3 | 79.5 | 89.1 | 39.0 | 48.6 | 59.3 | 67.6 | 79.6 |
| **12n** | 29.4 | 45.2 | 52.1 | 65.2 | 83.1 | 26.5 | 38.0 | 62.4 | 82.3 | 90.8 | 28.0 | 38.7 | 54.2 | 68.9 | 86.1 |
| **12o** | 26.9 | 36.9 | 49.3 | 64.9 | 84.5 | 31.0 | 41.8 | 58.3 | 81.9 | 89.4 | 38.0 | 50.8 | 66.6 | 80 | 93.6 |
| **Control** | 40.2 | 75.1 | 80.6 | 89.0 | 91.7 | 40.2 | 75.1 | 80.6 | 89.0 | 91.7 | 40.2 | 75.1 | 80.6 | 89.0 | 91.7 |

No*= Sample Code.
Std* = Ascorbic acid.

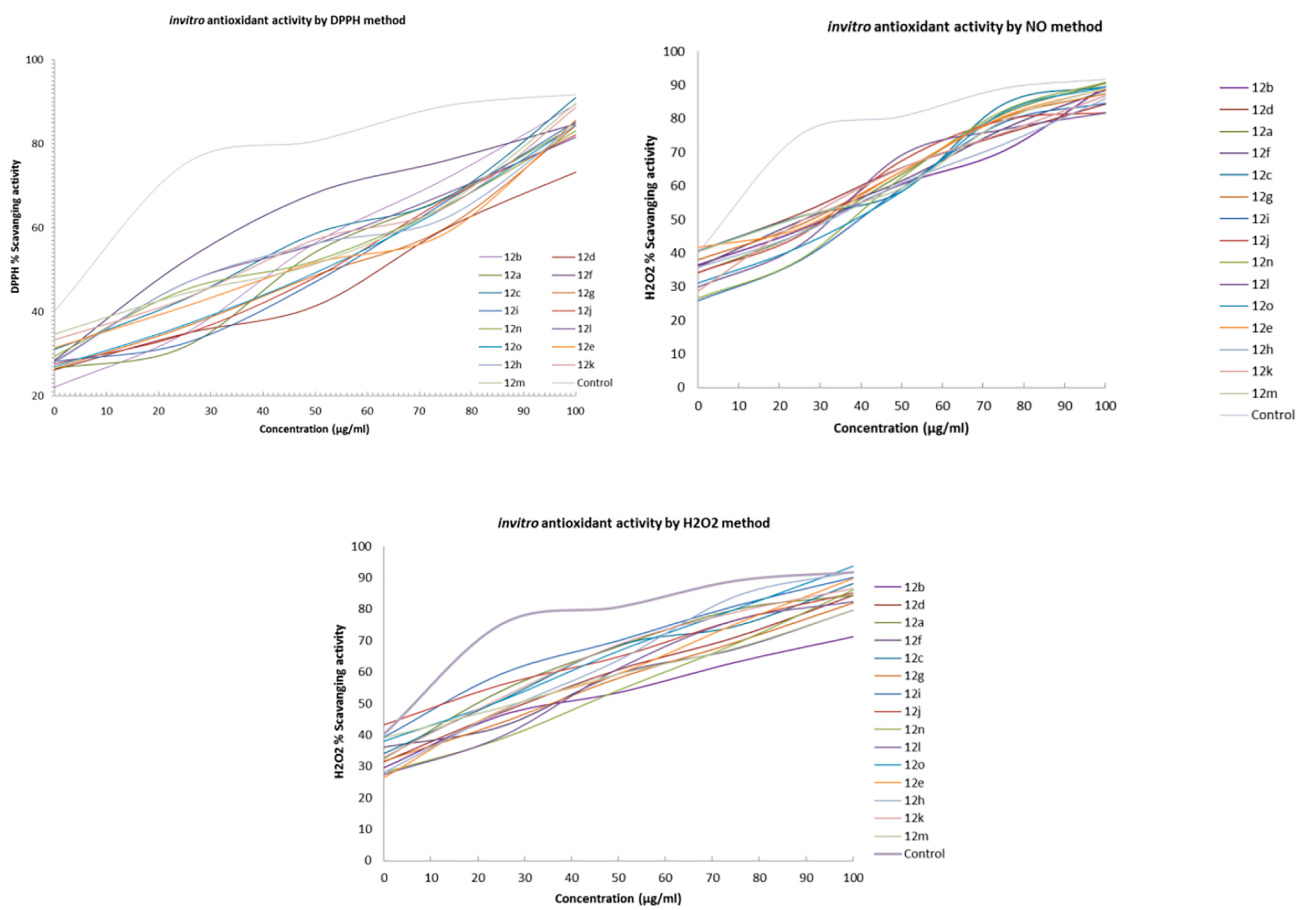


**Fig. 4.** Antioxidant activity of synthesized compounds.

evident that they show reducing ability. Among tested sample **12c** showed the most prominent scavenging capacity with 100 dilution value. Also, the activity is dose-dependent to scavenge the radical. From all tested compounds **12b,** and **12m** exhibited good antioxidant activity, with 100 dilution values in the range of 89.44 and 89.64 μg/ml, while 100 dilution value of ascorbic acid was 91.73 μg/ml, respectively.

In NO radical scavenging method, compounds **12a, 12b, 12c, 12m, 12o,** and **12n** displayed high activity as compared with the standard ascorbic acid. Compounds **12h,** and **12o** exhibited more potent activity against hydrogen peroxide as compared to standard reference. On the other hand, the compounds **12c,** and **12e** were less active. Similarly to previous DPPH assay compound **12b, 12c,** and **12m** showed to be the

**Table 5**
*In silico* Lipinski's rule of five properties of all compounds.

| Compound code | MW (130.0–725.0 gm/mol) | donorHB (<5) | accptHB (<10) | QPlogPo/w (<5) |
|---|---|---|---|---|
| **12a** | 450.404 | 2 | 9.7 | 2.191 |
| **12b** | 507.554 | 1 | 6.75 | 6.017 |
| **12c** | 524.008 | 1 | 6.75 | 6.499 |
| **12d** | 532.588 | 1 | 10.5 | 4.147 |
| **12e** | 540.463 | 1 | 6.75 | 6.923 |
| **12f** | 506.018 | 1 | 6.75 | 6.43 |
| **12g** | 471.573 | 1 | 6.75 | 6.043 |
| **12h** | 471.573 | 1 | 6.75 | 6.043 |
| **12i** | 505.544 | 1 | 9.75 | 4.048 |
| **12j** | 493.508 | 1 | 9 | 4.396 |
| **12k** | 554.414 | 1 | 9 | 4.779 |
| **12l** | 521.605 | 1 | 9.25 | 4.757 |
| **12m** | 509.569 | 1 | 8.5 | 4.874 |
| **12n** | 571.545 | 1 | 8.5 | 5.831 |
| **12o** | 554.447 | 1 | 8.5 | 5.697 |
| **sulfametoxydiazine** | 280.301 | 1 | 9 | 6.023 |
| **Sulfasalazine** | 398.392 | 1 | 8.25 | 2.467 |

MW: Molecular weight, donorHB: number of H bond donors,
accptHB: number of H bond acceptors, QPlogPo/w = log of the octanol–water partition coefficient.

more potent as a scavenger of NO method. Meanwhile, **12l** exhibited the weakest scavenging capacities in all the radical scavenging activity. Apart from this, the results also directed that radical scavenging activity in all the three methods increases with increase in concentration. Three methods of antioxidant activity were portrayed in graphically form in Fig 4.

A good number of *N*-based heterocyclic imidazole derivatives have been designed as probable antibacterial agents using *in silico* structure-based approach. The physicochemical data of all compounds and standard antibacterial agents were calculated using Schrodinger software. To find out the drug-like characteristics, molecules were evaluated using Lipinski's rule of five, which specifies that a probable drug molecule should have <5 log P, <500 Dalton molecular weight, <10 hydrogen bond acceptors and <5 hydrogen bond donor. As the rule of five compliance ensures the bioavailability, the molecules in the designed library were assumed to have better intestinal permeability. The presence of atoms allowed these molecules to function as H-bond acceptors as well as H-bond donors. The lipophilicity of log P of compounds was indicated that compounds should have no problem to passage through cell membrane. Therefore, results revealed that none of the designed ligand violated the rule of five and may be developed as potent drug-like antibacterial agents. The results summarized in Table 5 revealed that compounds possessed the drug-like characteristics, as standard antibacterial agents.

*In silico*, pharmacokinetics ADME parameters of all synthesized compounds with saDHPS protein (PDB ID: 6CLV) are predicted using Schrodinger software maestro 11.0 and summarized in Table 6. All the titled compounds have good percent of oral absorptions. Compound **12g, 12h,** and **12j** have 100% oral absorption, which is greater than reference drugs sulfametoxydiazine (69.708%) and Sulfasalazine (58.943%). All the compounds and standard drugs were found good results against the blood barrier potential, polar surface area, non-active transport QPPCaco, and QPlogKhsa in the permissible range. The aqueous solubility property was displayed moderate values of the analogous. Compound **12i** and reference drugs were showed good value in the permissible range. All ADME parameters including absorption, distribution, metabolism, and excretion were found to be favorable in the acceptable range for all the derivatives and in some cases, even better results than reference drugs were observed.

To study the binding of the designed ligands to the receptor binding site of saDHPS protein (PDB ID: 6CLV), a significant computational method, viz. molecular docking, was performed using Schrodinger maestro 11. All molecules **12a-12o** were docked within the active site of the receptor to evaluate the scoring functions and measure their mode of interactions. During the analysis of the results, compound **12a** showed the highest interaction energy, i.e. binding energy of **12a** was −51.288 kcal/mol, whereas compound **12h** displayed the lowest interaction energy, binding energy of **12h** was −38.000 kcal/mol. The rest of the compounds showed moderate binding free energy. Here, synthesized derivatives displayed the lowest binding free energy compared to the reference drug. During *in silico* studies, Dock Score (D.S.), again supported a better interaction of designed ligands with the protein DHPS. The designed imidazole derivatives showed significant to excellent dock score value ranging from −8.18 to −3.50, whereas sulfametoxydiazine, and Sulfasalazine exhibited dock score −5.29, and −4.843, respectively.

Molecular docking results were explained on the basis of hydrogen bonding and non-covalent interactions, which stabilized the ligand–-protein complex. Molecular docking results of all compounds with saDHPS protein were shown in Table 7. Docking results showed that compounds were accommodated well in the binding pocket of saDHPS. Standard marketed drugs Sulfasalazine formed four H-bonds with amino acids LYN203, ARG239, ARG219, and ARG204 and sulfametoxydiazine formed two H-bonds with amino acids ASN103, LYN203. A close inspection of docking results revealed that CONH group of all designed ligands formed 2 to 4-H bonds with amino acids. Compound **12l** formed H-bonds with amino acid ARG204, and GLY171; compound **12i** with

**Table 6**
ADME results of ligands with saDHPS receptor.

| Compound code | PHOA (>80% high, < 25% poor) | QPlogBB (−3.0 to 1.2) | QPPCaco (<25 poor, >500 great) | QPlogKhsa (−1.5 to 1.5) | PSA (70–200 Å) | QPlogS (−6.5 to 0.5) |
|---|---|---|---|---|---|---|
| **12a** | 90.965 | −0.988 | 1105.567 | 1.009 | 94.323 | −8.06 |
| **12b** | 89.86 | −0.846 | 988.084 | 0.99 | 87.366 | −8.045 |
| **12c** | 94.301 | −0.708 | 1217.029 | 1.124 | 84.679 | −8.681 |
| **12d** | 95.01 | −0.717 | 1477.303 | 1.055 | 91.171 | −8.101 |
| **12e** | 96.773 | −0.691 | 1214.874 | 1.253 | 83.9 | −9.403 |
| **12f** | 94.125 | −0.557 | 1695.736 | 0.947 | 73.97 | −7.442 |
| **12g** | 100 | −0.758 | 1875.59 | 0.989 | 80.343 | −7.883 |
| **12h** | 100 | −0.942 | 1024.378 | 0.948 | 85.165 | −7.707 |
| **12i** | 82.971 | −1.592 | 338.73 | 0.371 | 132.157 | −6.248 |
| **12j** | 100 | −1.397 | 392.507 | 0.462 | 123.277 | −6.87 |
| **12k** | 89.643 | −1.261 | 461.085 | 0.55 | 121.11 | −7.383 |
| **12l** | 88.615 | −1.418 | 410.418 | 0.596 | 121.655 | −7.064 |
| **12m** | 88.359 | −1.308 | 363.722 | 0.643 | 115.073 | −7.334 |
| **12n** | 83.043 | −0.988 | 507.723 | 0.866 | 110.324 | −8.241 |
| **12o** | 81.693 | −1.112 | 439.592 | 0.879 | 112.624 | − 8.334 |
| **sulfametoxydiazine** | 69.708 | −1.374 | 209.539 | −0.696 | 106.593 | −2.401 |
| **Sulfasalazine** | 58.943 | −2.659 | 9.567 | −0.29 | 152.039 | −4.679 |

**Table 7**
Docking results: molecular docking interaction of ligands with saDHPS receptor.

| Compound code | Docking score | Gevdw | No. of H-B/Amino acid in H-B (distance Å) | No. of π-B/Amino acid in π-B |
|---|---|---|---|---|
| **12a** | −7.69 | −51.288 | 2/ARG204 (2.23), GLY171 (2.26) | 4/ARG176, PHE172, ARG52, ARG204 |
| **12b** | −6.67 | −42.625 | 2/ARG204 (2.22), GLY171 (2.18) | 5/ARG52, PHE172, PHE172, ARG204, ARG176 |
| **12c** | −6.54 | −46.741 | 3/ARG176 (1.86), ARG204 (2.20), GLY171 (2.37) | 5/ARG52, PHE172, PHE172, ARG176, ARG204 |
| **12d** | −7.43 | −48.993 | 4/ARG204 (2.18), GLY171 (2.41), ASH84 (1.99), GLY54 (2.07) | 1/ARG52 |
| **12e** | −6.52 | −46.511 | 3/ARG176 (2.06), ARG204 (2.18), GLY171 (2.39) | 4/ARG52, PHE172, ARG176, ARG204 |
| **12f** | −5.34 | −46.332 | 3/ARG176 (1.96), ARG204 (2.34), GLY171 (2.28) | 3/ARG52, PHE172, PHE172 |
| **12g** | −3.50 | −45.667 | 3/ARG176 (1.98), ARG204 (2.32), GLY171 (2.28) | 3/ARG52, PHE172, PHE172 |
| **12h** | −5.27 | −38.000 | 2/ARG176 (2.01), ARG204 (2.20) | 5/ARG204, ARG176, ARG52, ARG52, PHE172 |
| **12i** | −8.18 | −44.905 | 4/ARG176 (1.91), ARG204 (2.21), GLY171 (2.18), ARG239 (2.39) | 6/ARG176, ARG204, ARG52, PHE172, ARG52, PHE172 |
| **12j** | −5.89 | −47.837 | 4/ARG176 (2.02), ARG204 (2.30), GLY171 (2.34), ARG239 (2.53) | 5/ARG176, ARG204, ARG52, PHE172, PHE172 |
| **12k** | −6.22 | −44.67 | 2/GLY171 (2.22), ARG204 (2.27) | 4/PHE172, ARG52, ARG176, ARG204 |
| **12l** | −6.57 | −49.217 | 2/ARG204 (2.41), GLY171 (2.12) | 4/ARG52, PHE172, ARG52, ARG204 |
| **12m** | −6.94 | −44.471 | 2/ARG204 (2.25), ARG239 (2.59) | 5/ARG204, ARG176, ARG52, PHE172, PHE172 |
| **12n** | −7.55 | −49.926 | 3/GLY54 (1.99), ARG204 (2.18), GLY171 (2.60) | 3/PHE172, PHE172, ARG52 |
| **12o** | −7.51 | −47.158 | 3/ARG176 (1.86), ARG204 (2.24), GLY171 (2.29) | 4/ARG204, ARG176, ARG52, PHE176 |
| **sulfametoxydiazine** | −5.29 | −35.694 | 2/ASN103 (2.04), LYN203 (2.12) | 3/ARG52, PHE172, PHE172 |
| **Sulfasalazine** | −4.843 | −30.136 | 4/LYN203 (2.20), ARG239 (2.31), ARG219 (2.16), ARG204 (2.12) | 1/ARG204 |

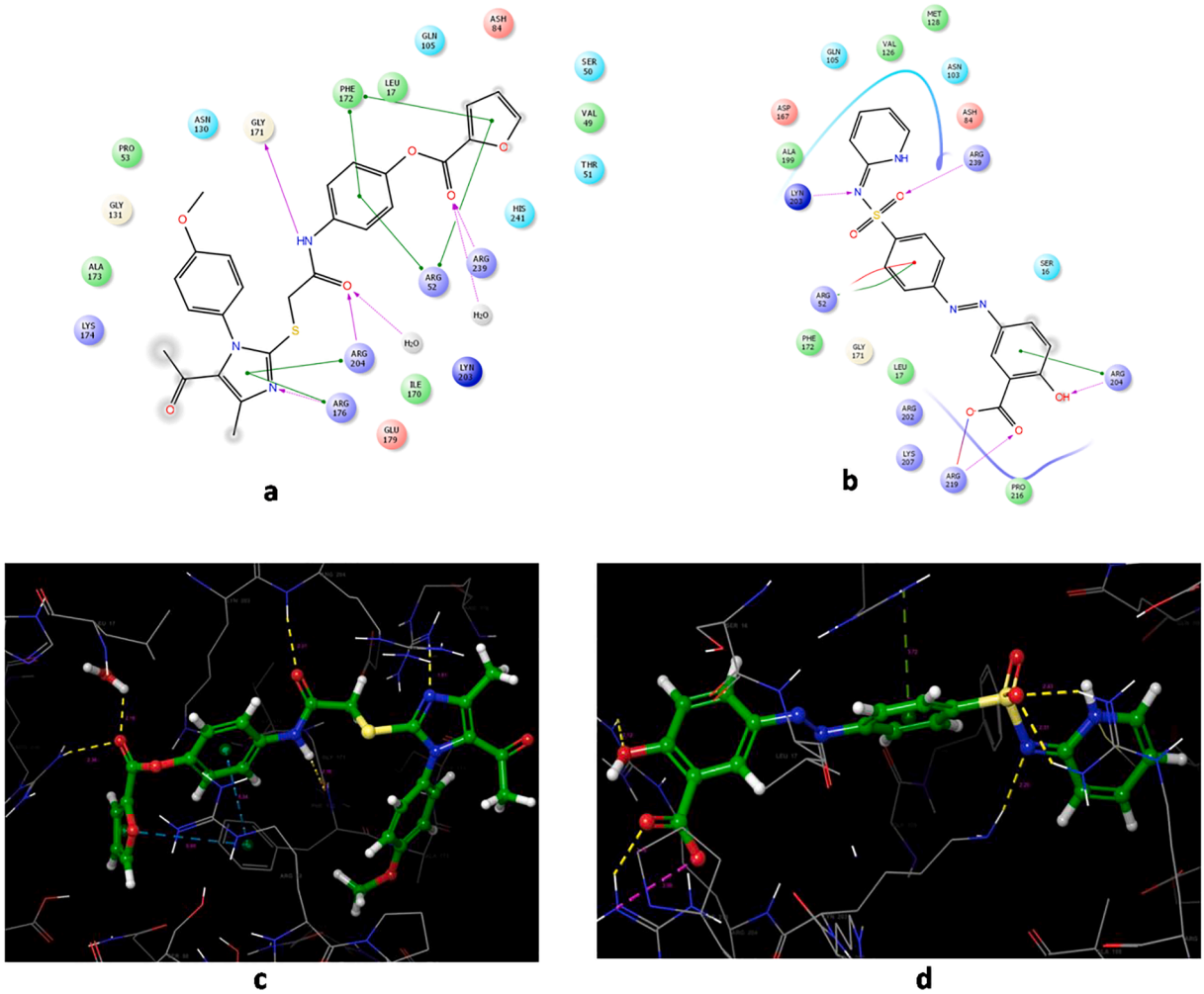


**Fig. 5.** a and b are 2D binding pose and c and d are 3D binding pose of compounds **12i** and **sulfasalazine**, respectively (PDB ID: 6CLV).

ARG176, ARG204, GLY171, and ARG239.

Most notably, docking results revealed that all compounds interacted with the active site of saDHPS enzyme and formed 2 to 6 π-π interactions with amino acid residues. Sulfasalazine formed one π-π interaction with ARG204 amino acid while sulfametoxydiazine interacted with ARG52, PHE172, and PHE172 to form π-π interactions. Compound **12i** showed six π-π interactions with ARG176, ARG204, ARG52, PHE172, ARG52, and PHE172. Analogous **12l** displayed 4 π-π interactions with ARG204, ARG52, PHE172, and ARG52. **12b, 12c,** and **12m** showed the same π-π interactions with ARG52, PHE172, PHE172, ARG204, and ARG176. Compounds, additionally, showed two π-π interactions with ARG176, and ARG204, which was not observed in reference drugs. Molecular

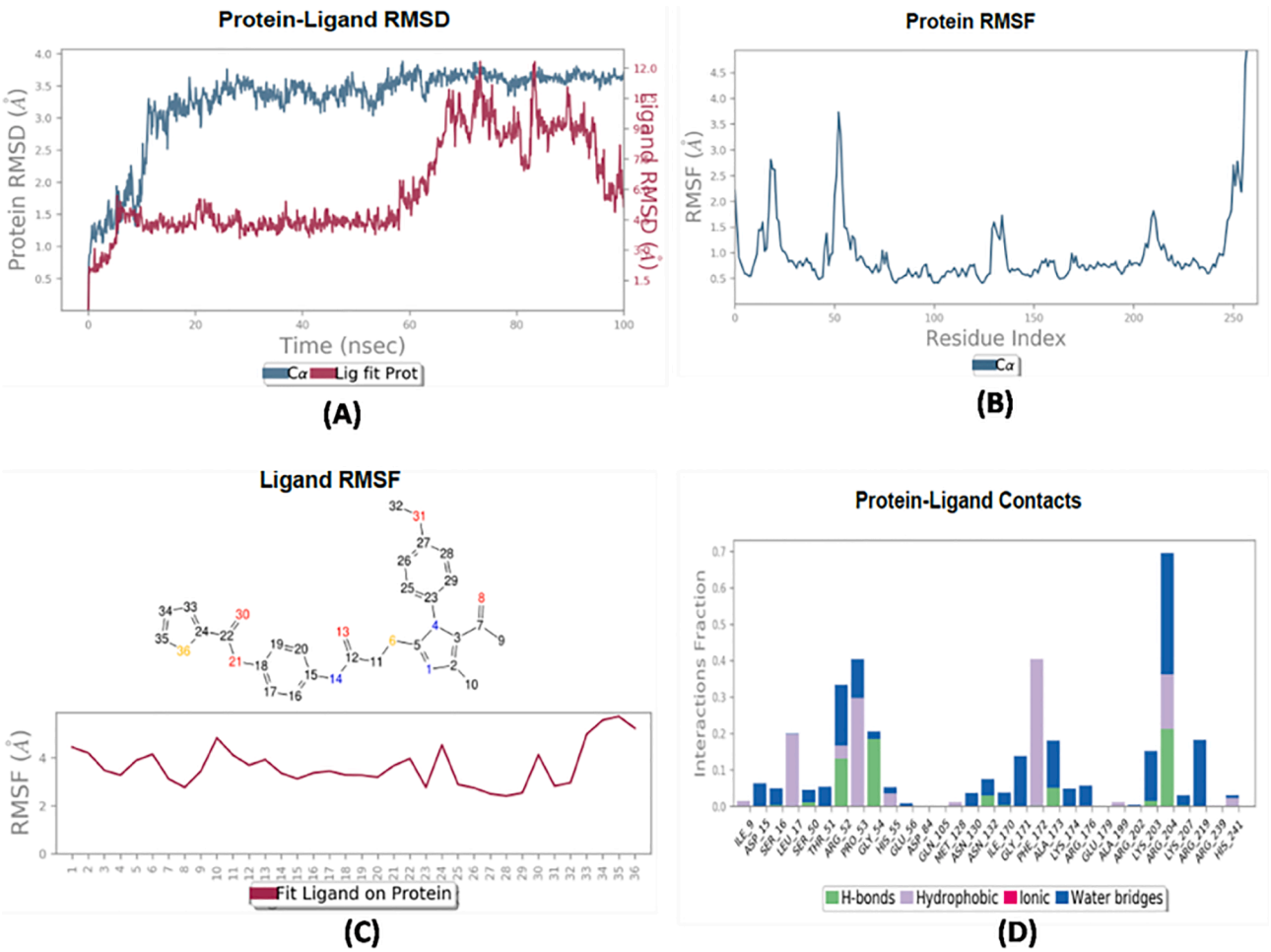


**Fig. 6.** (A) RMSD (B) Protein RMSF (C) Ligand RMSF and (D) Protein-Ligand Contacts of protein 6CLV-compound **12 l** complex during the MD simulations of 100 ns.

docking interactions of some selected imidazole derivatives and the reference drugs with the active site of saDHPS binding pocket are shown in Fig 5.

MD simulation offered to probe the behavioral dynamics of biomacromolecules including protein–ligand complex from nanometer to micrometer timescales. In this study, the MD simulation of the ligand–protein complex was considered to explore in detail of interactions of ligand **12l** with saDHPS enzyme (PDB ID: 6CLV) individually at a 100 ns. The Root Mean Square Deviation (RMSD) of the enzyme backbone with rapidly increased up to 3.0 Å during the initial 15 ns (ns) then a relatively constant value of 3.0–3.5 Å for the rest of the trajectory. Moreover, the Ligand RMSD of all system initially increased up to 4.5 Å during 10 ns then stable up to 60 ns after that increased value with fluctuation which ends at 6.0 Å (Fig. 6A). On this RMSF plot, peaks indicated area of the protein that fluctuates the most during the simulation. Typically, the plot was observed that the tails (N- and C-terminal) fluctuated more than any other part of the protein. Secondary structure elements like alpha helices and beta strands were usually more rigid than the unstructured part of the protein, and thus fluctuate less than the loop regions (Fig. 6B). Ligand RMSF showed the ligand's fluctuations broken down by atom, corresponding to the 2D structure in the top panel. In the bottom panel, the 'Fit Ligand on Protein' line displayed the ligand fluctuations, concerning the protein (Fig. 6C).

For scrutinization of intermolecular H-bonding patterns in the saDHPS-compound **12l** complex was not displayed in the system. The protein–ligand contacts during the simulation, a few H-bonds were found during contacts; hence, ionic bonds were not shown in the complex. Compound **12l** was exhibited H-bond, hydrophobic, and water bridge interaction in the stable region of ARG-52, and ARG-204. H-bond found to be formed majorly with ARG-52, GLY-54, ALA-173, ARG-204, and hydrophobic interaction was dominated by SER-16, PRO-53, PHE-172, ARG-204 throughout the dynamic simulation. The residues of ASP-84, GLN-105, GLU-179, and ARG-239 were not found any interaction due to fluctuation (Fig 6D). A mean RMSD of 2.5 Å of compound indicated good conformational modification; high polar solvent area (PSA) (105–135 Å), solvent accessible surface area (SASA) (150–600), and molecular surface area (MolSA) (420–460 Å) of the compound during simulation time which is further supported its stabilization during 100 ns molecular dynamic simulation (Fig. 7).

In summary, all the synthesized compounds with imidazole scaffold were prepared and evaluated for their *in vitro* antimicrobial activity including drug-resistant strains were assessed in this work. We have synthesized novel compounds for saDHPS enzyme target, including MRSA, ESBL, and VRE. Among all the compounds, compound **12l** (MIC = 62.5, 100, 100 μg/mL) exhibited broad-spectrum antibacterial activity against all ESBL, VRE, and MRSA strains, respectively. The SAR

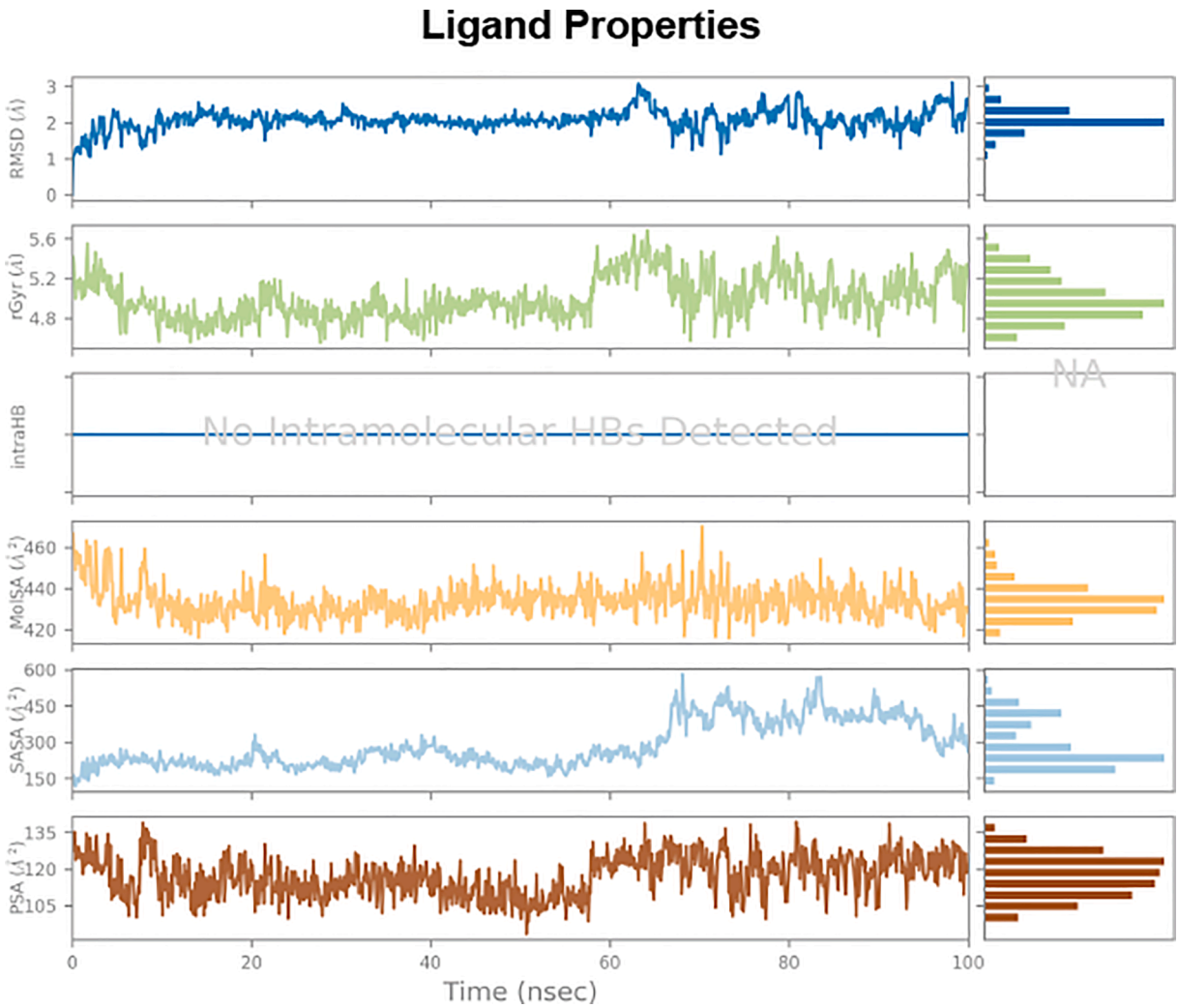


**Fig. 7.** Ligand properties of the protein–ligand complex during the MD simulations of 100 ns.

revealed that the substituent $OCH_3$ at 4th position resulted in potency against resistant bacterial strains. In addition, compound **12a** (MIC = 25 μg/mL) as efficacious against ESBL strain. Meanwhile, *in silico* study confirmed that all the compounds possessed good docking scores between −8.18 to −3.50, and found drug-likeness properties. Furthermore, all the compounds were tested for their *in vitro* antituberculosis, antimalarial, antioxidant activities. Hence, analogous **12h, 12l** ($IC_{50}$ = 0.45 μg/mL), 12j ($IC_{50}$ = 0.36 μg/mL) were exhibited good activity as compared with reference drug Quinine (0.268 μg/mL).

## Declaration of Competing Interest

The authors declare that they have no known competing financial interests or personal relationships that could have appeared to influence the work reported in this paper.

## Acknowledgements

The authors are thankful to the Department of Chemistry, Gujarat University Ahmedabad, for providing the necessary facilities. UGC-Info net & INFLIBNET Gujarat University are acknowledged for providing the e-resource facilities, NFDD Centre for $^1$H NMR and AnSys Research Laboratories for mass spectroscopy. Authors are thankful to Microcare laboratory for biological screening. We are very much thankful to Schrodinger team for the computational tools.

## Appendix A. Supplementary data

Supplementary data to this article can be found online at https://doi.org/10.1016/j.bmcl.2021.127819.

## References

1 Dolan N, Gavin DP, Eshwika A, Kavanagh K, McGinley J, Stephens JC. Synthesis, antibacterial and anti-MRSA activity, in vivo toxicity and a structure–activity relationship study of a quinoline thiourea. *Bioorg Med Chem Lett.* 2016;26(2):630–635.
2 Naaz F, Srivastava R, Singh A, et al. Molecular modeling, synthesis, antibacterial and cytotoxicity evaluation of sulfonamide derivatives of benzimidazole, indazole, benzothiazole and thiazole. *Bioorg Med Chem.* 2018;26(12):3414–3428.
3 Chavan RR, Hosamani KM, Kulkarni BD, Joshi SD. Molecular docking studies and facile synthesis of most potent biologically active N-tert-butyl-4-(4-substituted phenyl)-2-((substituted-2-oxo-2H-chromen-4-yl) methylthio)-6-oxo-1, 6-dihydropyrimidine-5-carboxamide hybrids: an approach for microwave-assisted syntheses and biological evaluation. *Bioorg Chem.* 2018 Aug;1(78):185–194. https://doi.org/10.1016/j.bioorg.2018.03.007.
4 El-Attar MAZ, Elbayaa RY, Shaaban OG, et al. Design, synthesis, antibacterial evaluation and molecular docking studies of some new quinoxaline derivatives targeting dihyropteroate synthase enzyme. *Bioorg Chem.* 2018;76:437–448.
5 Hevener KE, Yun M-K, Qi J, Kerr ID, Babaoglu K, et al. Structural studies of pterin-based inhibitors of dihydropteroate synthase. *J Med Chem.* 2010;53(1):166–177.
6 Nasr T, Bondock S, Eid S. Design, synthesis, antimicrobial evaluation and molecular docking studies of some new 2,3-dihydrothiazoles and 4-thiazolidinones containing sulfisoxazole. *J Enzyme Inhib Med Chem.* 2016;31(2):236–246.
7 Zhang L, Kumar KV, Rasheed S, Geng R-X, Zhou C-H. Design, synthesis, and antimicrobial evaluation of novel quinolone imidazoles and interactions with MRSA DNA. *Chem Biol Drug Des.* 2015;86(4):648–655.

8 Coelho C, de Lencastre H, Aires-de-Sousa M. Frequent occurrence of trimethoprim-sulfamethoxazole hetero-resistant Staphylococcus aureus isolates in different African countries. *Eur J Clin Microbiol Infect Dis.* 2017;36(7):1243–1252.

9 Dennis ML, Pitcher NP, Lee MD, DeBono AJ, Wang Z-C, Harjani JR, Rahmani R, et al. Structural basis for the selective binding of inhibitors to 6-hydroxymethyl-7,8-dihydropterin pyrophosphokinase from staphylococcus aureus and Escherichia coli. *J Med Chem.* 2016;59(11):5248–5263.

10 Patel BA, Ashby Jr CR, Hardej D, Talele TT. The synthesis and SAR study of phenylalanine-derived (Z)-5-arylmethylidene rhodanines as anti-methicillin-resistant Staphylococcus aureus (MRSA) compounds. *Bioorg Med Chem Lett.* 2013;23(20):5523–5527.

11 Dennis ML, Chhabra S, Wang Z-C, Debono A, Dolezal O, Newman J, Pitcher NP, Rahmani R, Cleary B, Barlow N, Hattarki M, et al. Structure-based design and development of functionalized mercaptoguanine derivatives as inhibitors of the folate biosynthesis pathway enzyme 6-hydroxymethyl-7,8-dihydropterin pyrophosphokinase from staphylococcus aureus. *J Med Chem.* 2014;57(22):9612–9626.

12 Keshipeddy S, Reeve SM, Anderson AC, Wright DL. Nonracemic antifolates stereoselectively recruit alternate cofactors and overcome resistance in S. aureus. *J Am Chem Soc.* 2015;137(28):8983–8990.

13 Ghosh S, Prava J, Samal HB, Suar M, Mahapatra RK. Comparative genomics study for the identification of drug and vaccine targets in Staphylococcus aureus: MurA ligase enzyme as a proposed candidate. *J Microbiol Methods.* 2014 Jun;1(101):1–8. https://doi.org/10.1016/j.mimet.2014.03.009.

14 Swain SS, Paidesetty SK, Padhy RN. Antibacterial, antifungal and antimycobacterial compounds from cyanobacteria. *Biomed Pharmacother.* 2017 Jun;1(90):760–776. https://doi.org/10.1016/j.biopha.2017.04.030.

15 Stratton CF, Namanja-Magliano HA, Cameron SA, Schramm VL. Binding isotope effects for para -aminobenzoic acid with dihydropteroate synthase from staphylococcus aureus and plasmodium falciparum. *ACS Chem Biol.* 2015;10(10):2182–2186.

16 Das BK, Pushyaraga PV, Chakraborty D. Computational insights into factor affecting the potency of diaryl sulfone analogs as Escherichia coli dihydropteroate synthase inhibitors. *Comput Biol Chem.* 2019 Feb;1(78):37–52. https://doi.org/10.1016/j.compbiolchem.2018.11.005.

17 Griffith EC, Wallace MJ, Wu Y, Kumar G, Gajewski S, Jackson P, Phelps GA, Zheng Z, Rock CO, Lee RE, White SW. The structural and functional basis for recurring sulfa drug resistance mutations in Staphylococcus aureus dihydropteroate synthase. *Front Microbiol.* 2018 Jul;17(9):1369. https://doi.org/10.3389/fmicb.2018.01369.

18 Wang Z, Liang X, Wen K, Zhang S, Li C, Shen J. A highly sensitive and class-specific fluorescence polarisation assay for sulphonamides based on dihydropteroate synthase. *Biosens Bioelectron.* 2015 Aug;15(70):1–4. https://doi.org/10.1016/j.bios.2015.03.016.

19 Dennis ML, Lee MD, Harjani JR, Ahmed M, DeBono AJ, Pitcher NP, Wang Z-C, Chhabra S, Barlow N, Rahmani R, Cleary B, Dolezal O, Hattarki M, Aurelio L, Shonberg J, et al. 8-Mercaptoguanine derivatives as inhibitors of dihydropteroate synthase. *Chem Eur J.* 2018;24(8):1922–1930.

20 Zhao Y, Hammoudeh D, Lin W, Das S, Yun M-K, Li Z, et al. Development of a pterin-based fluorescent probe for screening dihydropteroate synthase. *Bioconjugate Chem.* 2011;22(10):2110–2117.

21 Zhao Y, Shadrick WR, Wallace MJ, Wu Y, Griffith EC, et al. Pterin–sulfa conjugates as dihydropteroate synthase inhibitors and antibacterial agents. *Bioorg Med Chem Lett.* 2016;26(16):3950–3954.

22 Li C, Liang X, Wen K, Li Y, Zhang X, Ma M, et al. Class-specific monoclonal antibodies and dihydropteroate synthase in bioassays used for the detection of sulfonamides: structural insights into recognition diversity. *Anal Chem.* 2019;91(3):2392–2400.

23 Nasr T, Bondock S, Ibrahim TM, et al. New acrylamide-sulfisoxazole conjugates as dihydropteroate synthase inhibitors. *Bioorg Med Chem.* 2020;28(9):115444. https://doi.org/10.1016/j.bmc.2020.115444.

24 Pemble IV CW, Mehta PK, Mehra S, Li Z, Nourse A, Lee RE, White SW. Crystal structure of the 6-hydroxymethyl-7, 8-dihydropterin pyrophosphokinase• dihydropteroate synthase bifunctional enzyme from Francisella tularensis. *PloS One.* 2010 Nov 30;5(11). https://doi.org/10.1371/journal.pone.0014165.

25 Hammoudeh DI, Daté M, Yun M-K, Zhang W, Boyd VA, Viacava Follis A, et al. Identification and characterization of an allosteric inhibitory site on dihydropteroate synthase. *ACS Chem Biol.* 2014;9(6):1294–1302.

26 Capasso C, Supuran CT. Sulfa and trimethoprim-like drugs – antimetabolites acting as carbonic anhydrase, dihydropteroate synthase and dihydrofolate reductase inhibitors. *J Enzyme Inhib Med Chem.* 2014;29(3):379–387.

27 Fernley RT, Iliades P, Macreadie I. A rapid assay for dihydropteroate synthase activity suitable for identification of inhibitors. *Anal Biochem.* 2007;360(2):227–234.

28 Azzam RA, Elsayed RE, Elgemeie GH. Design, synthesis, and antimicrobial evaluation of a new series of N -sulfonamide 2-pyridones as dual inhibitors of DHPS and DHFR enzymes. *ACS Omega.* 2020;5(18):10401–10414.

29 Gotthard G, Muhammed Ameen S, Drancourt M, Chabriere E. Long-range DHPS mutations unexpectedly increase Mycobacterium chimaera susceptibility to sulfonamides. *J Glob Antimicrob Resist.* 2013;1(4):181–188.

30 Sánchez-Osuna M, Cortés P, Barbé J, Erill I. Origin of the mobile di-hydro-pteroate synthase gene determining sulfonamide resistance in clinical isolates. *Front Microbiol.* 2019 Jan;10(9):3332. https://doi.org/10.3389/fmicb.2018.03332.

31 Mondal S, Mandal SM, Mondal TK, Sinha C. Spectroscopic characterization, antimicrobial activity, DFT computation and docking studies of sulfonamide Schiff bases. *J Mol Struct.* 2017 Jan;5(1127):557–567. https://doi.org/10.1016/j.molstruc.2016.08.011.

32 Eliopoulos GM, Huovinen P. Resistance to trimethoprim-sulfamethoxazole. *Clin Infect Dis.* 2001;32(11):1608–1614.

33 Zhao Y, Hammoudeh D, Yun M-K, Qi J, White SW, Lee RE. Structure-based design of novel pyrimido[4,5-c]pyridazine derivatives as dihydropteroate synthase inhibitors with increased affinity. *ChemMedChem.* 2012;7(5):861–870.

34 Ghorab MM, Soliman AM, Alsaid MS, Askar AA. Synthesis, antimicrobial activity and docking study of some novel 4-(4,4-dimethyl-2,6-dioxocyclohexylidene) methylamino derivatives carrying biologically active sulfonamide moiety. *Arabian J Chem.* 2020;13(1):545–556.

35 Mondal S, Mandal SM, Mondal TK, Sinha C. Structural characterization of new Schiff bases of sulfamethoxazole and sulfathiazole, their antibacterial activity and docking computation with DHPS protein structure. *Spectrochim Acta Part A Mol Biomol Spectrosc.* 2015 Nov;5(150):268–279. https://doi.org/10.1016/j.saa.2015.05.049.

36 Gill RK, Singh H, Raj T, Sharma A, Singh G, Bariwal J. 4-Substituted thieno[2,3- d ] pyrimidines as potent antibacterial agents: rational design, microwave-assisted synthesis, biological evaluation and molecular docking studies. *Chem Biol Drug Des.* 2017;90(6):1115–1121.

37 Z El-Attar MA, Elbayaa RY, Shaaban OG, et al. Synthesis of pyrazolo-1,2,4-triazolo [4,3- a ]quinoxalines as antimicrobial agents with potential inhibition of DHPS enzyme. *Future Med Chem.* 2018;10(18):2155–2175.

38 Hammoudeh DI, Zhao Y, White SW, Lee RE. Replacing sulfa drugs with novel DHPS inhibitors. *Future Med Chem.* 2013;5(11):1331–1340.

39 Dhawas AK, Thakare SS. Synthesis of some new imidazole-2-thiols and their derivatives as potent antimicrobial agents. *Ind J Chem.* 2014 May;53:642–646. http://hdl.handle.net/123456789/28753.